Dosimetric comparison between proton and carbon ion beams for oncological treatments using Monte Carlo methods

Carlos Correia*

Radiotherapy is one of the main treatments for cancer. During the last decade, its focus has shifted towards proton or carbon radiotherapy. The properties of particle radiotherapy allow for a specific dose distribution, errors in the range of the particles can lead to underdosage to the tumour or overdosage to healthy organs.

This work aims at quantifying the differences in range caused by missassignment errors in the Computed Tomography (CT) of a patient. Dose profiles were obtained using Monte Carlo (MC) *software* TOolkit for PArticle Simulation (TOPAS) and the plan parameters were optimized using matRad, an open source code based on MATLAB. The beams were validated with an average range difference of (0.4±0.3) mm.

A treatment for a brain tumour of a pediatric patient was developed. Segmentation errors were introduced by modifying the method of conversion from Hounsfield Units (HU) in the CT to densities and compositions. Voxels of the CT, either with muscle or adipose tissue, kept their composition but were assigned the density of water. This allows the study of the impact of changes on the density on the range.

The average difference in range was 3.5 mm (2.6 % of the range) with a standard deviation of 0.4 mm, this is the worst case scenario.

The calculations regarding carbon radiotherapy could not be finished due to long computational times. Nevertheless taking into account the validation and physics of these beams, the difference in range is expected to be similar or inferior to the one calculated for protons.

I. INTRODUCTION

Cancer represents a group of diseases, which can affect any part of the human body. Cancer originates from the formation of abnormal cells within a tissue or organ, which happens due to interactions between an individual's genetic factors and external agents. These abnormal cells grow rapidly and beyond their supposed boundaries, they can invade adjacent parts of the body and consequently other organs or tissues, a process known as metastasis [1].

In 2018 there were more than 18 million new instances of cancer worldwide and the disease lead to almost 10 million deaths [2]. Cancer, in 2018, ranked as the second leading cause of death worldwide [1]. These numbers are expected to rise to nearly 30 million new instances in 2040 leading to more than 16 million casualties.

Due to the increase in both new instances and fatalities caused by cancer, several therapies are used for treatment of the disease, namely surgery, radiotherapy and chemotherapy. All these therapies have the same end goal, destroying the cancer cells, while trying to minimize the damage to healthy ones [3]. Radiotherapy has been estimated as being beneficial to about 50% of cancer patients [4].

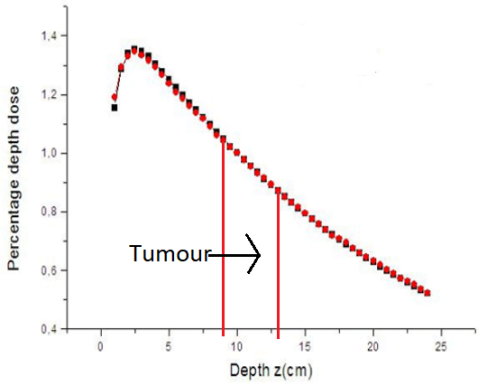

Figure 1: Photon dose distribution in a water phantom. Adapted from [7].

In Portugal, in 2018 there were 58 thousand new cases of cancer and they lead to 29 thousand deaths. Currently, there is a 10.6% chance of dying of cancer before the age of 75, a higher indicator than the 9.7% of the neighbour Spain which has recently (opened 1 clinic in 2019 and another in 2020) started using proton radiotherapy. Taking these numbers and the fact that Portugal has not yet invested into this type of treatment, perhaps it is time to invest in particle radiotherapy to enhance cancer treatment. [5, 6].

Photons are massless particles. Their energy is deposited as the beam moves through the body. Because of this, the dose delivered will decrease as the depth of

* carlos.e.correia@tecnico.ulisboa.pt

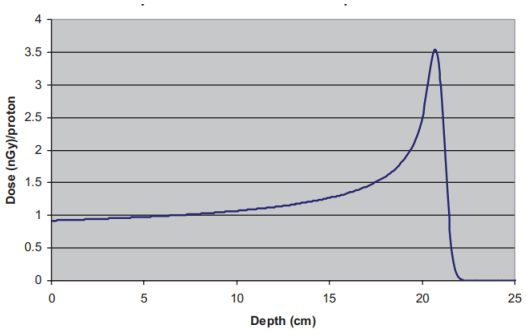

Figure 2: Proton dose distribution showing the Bragg peak. Adapted from [8].

penetration increases, which causes the dose to be at its highest where the beam enters the body. Another consequence is that healthy tissues that are geometrically before the tumour would receive a dose higher than the tumour itself, as can be seen in Figure 1. Due to the way photons interact with matter photon radiotherapy has intrinsic limitations.

In 1903, Bragg discovered that light charged particles deposit their energy in a different way. They deposit little energy during most of their path until finally they have a peak, before stopping, where they deposit most of their energy. This originates a well defined peak, known as the Bragg peak, which is depicted in Figure 2.

Since the goal of proton therapy is to deliver dose in a very specific configuration, errors in the range of the beams are much more severe than in photon radiotherapy. Therefore, to accurately develop a treatment plan the effects that cause these uncertainties must be understood and fully quantified.

There are uncertainties inherent to the statistical nature of range and proton interactions. The incident beam is not monoenergetic, therefore the lower energy protons will have shorter range while higher energy protons will deposit their energy at a larger depth. Proton interactions with matter are governed by probability and the energy lost by each single proton will vary, these uncertainties are uncontrollable. Organ motion also has to be taken into account. This thesis focused on changes in the patients anatomy in the period between the planning of the treatment and the delivery and uncertainties in the CT numbers. Both of these errors cause missassignments in the tissues. In fact, the material defined by the CT for a voxel of the patient will not be the actual material in that position.

In this work, Monte Carlo (MC) simulations were used to quantify the impact of these missassignment errors in the CT on the dose delivered to the patient. MC methods have similarities between them. Source of particles, treatment head (which includes all the machinery required to deliver the beam, range shifters, collimators, etc) and finally the patient itself must be modeled and all relevant particles must be tracked. Each particle is tracked by calculating its position at each step of the simulation and, considering the cross sections for all possible interactions, what interaction it will undergo, if any. Particles are tracked until their energy reaches a certain threshold and then deposit their energy in that position. MC simulations are inherently statistical, as are particle interactions with matter.

All simulations in this thesis were based on a Geant4 code [9], TOolkit for PArticle Simulation (TOPAS), developed by TOPAS MC Inc for particle therapy interactions and in close collaboration with particle therapy centers[10]. It is very important to mention that this code is for research purposes only.

Geant4 is a 4D simulation software that can handle time dependent variables, such as organ motion or moving components during treatment. TOPAS is a complex interface built on top of the of Geant4 libraries allowing TOPAS to evolve and derive from it [11].

One of the main advantages of TOPAS is that the user does not have to work with the underlying code. To run simulations it is only necessary to create parameter files, these parameter files specify all the variables of the simulation such as the geometry, source of particles, patient, and physics. A capability of TOPAS which will be very useful for this work is the possibility of inheriting parameters from other files. This helps in keeping the files organized and facilitates the implementation.

The final goal of the work is to quantify the impacts of missassginment errors in the CT of a patient on the delivered dose in a treatment plan and infer about the clinically used margins. Too large margins lead to an unnecessary amount of normal tissue being irradiated. This work will also compare the results between proton and carbon ion radiotherapy and discuss the differences between the two as well as the advantages and disadvantages of each.

II. VALIDATION

A. Motivation

The process of creating a treatment plan with particle therapy requires defining several parameters that follow detailed clinical protocols which depend on the type of particle, beam, machine and even center. In particular, the treatment plan is calculated by complex algorithms that manipulate parameters such as spot position and size as well as beam energy and weight to achieve the best possible dose to the target while minimizing dose delivered to the surrounding volumes.

In this thesis, an open-source research software named matRad developed by German Cancer Research Center in the Helmholtz association was used as a tool to create the treatment plan that would later be simulated with Monte Carlo dose engine. matRad is a software developed in MATLAB with a graphical user interface which allows the user to easily input a set of variables and parameters and gives a treatment plan as the final result. The full matRad flowchart can be seen in Figure 3. The

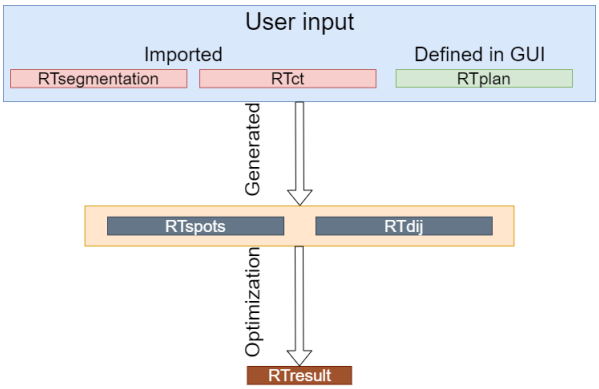

Figure 3: matRad flowchart for a treatment plan.

first two variables, which can be imported, are the *cst* struct (RTsegmentation) which stores information about the regions of interest and the *ct* struct (RTct) that holds the CT of the phantom or pacient, having the Hounsfield units for each voxel as well as the resolution and dimensions, italic names refer to matRad variables. The next step is defining the treatment plan parameters, this information will be stored in the *pln* struct (RTplan) and includes the chosen particle and machine for the treatment as well as the gantry and couch angles which are to be used, the separation between scanning spots and the type of optimization that will be ran further ahead. Using RTsegmentation, RTct and RTplan matRad generates the *stf* struct (RTspots) that holds information about the spacial distribution of the spots and the *dij* struct (RTdij) which contains the contributions to dose of each beam and the initial dose. Finally, by inverse planning and iterative functions the dose is optimized, taking into account the constraints and objectives set in RTplan, to achieve the minimum difference between planned and delivered dose, the result is stored in the *resultGUI* struct (RTresult) and contains the dose distribution as well as the weights to be used for each beam.

B. Single Beams

To be able to run the treatment plan created in matRad in TOPAS the beams in the matRad machine have to be validated, as explained here. The chosen machine consists of 86 generic beams with energies ranging from 73.4 MeV to 216.4 MeV corresponding to , accordingly, to ranges in water (R_{80}) of 44.97 mm to 298.84 mm covering clinical ranges. The dose distributions for each of these beams are calculated using the analytical model described in [12].

The validation consisted of simulating proton beams with no initial energy spread travelling through a cubic water phantom divided into 0.5 mm voxels, as shown in Figure 4. The size of the phantom changed for each energy taking into account the necessary dimension to be able to score the relevant zones of the dose distribution

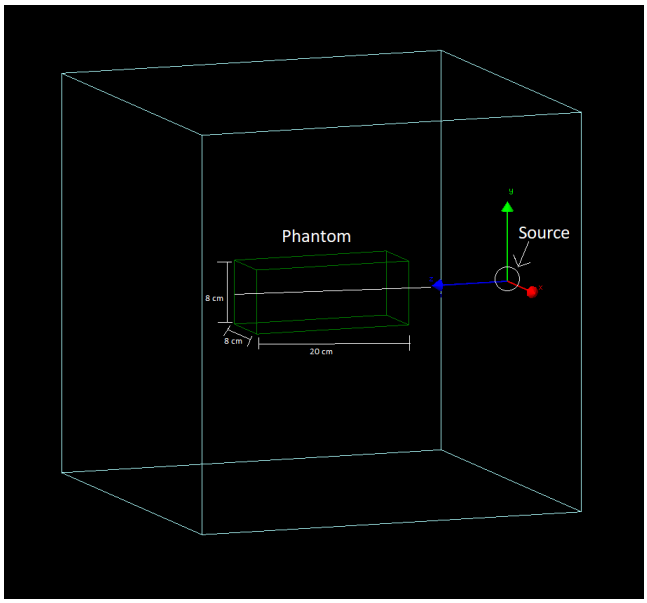

Figure 4: General setup for the simulations for the validation of the 86 beams.

(entrance, plateau, Bragg Peak and distal falloff) using TOPAS default physics settings and obtaining the integrated dose/depth distribution of each beam. The dose distribution is then compared with the one from corresponding beam in the matRad machine.

To adjust the beams, the energy was used as a free parameter and changed until the difference in range (R_{80}) from the simulated beams and the corresponding MatRad ones was smaller than 1 mm (2 voxels), although preferably errors would be within 0.5 mm (1 voxel). The process of reducing this difference is extremely time consuming and 1 mm is within the margins considered by clinics when creating a treatment plan, which are 3.5% of the range of the beam plus 1 to 3 mm (depending on the clinic) [13].Each beam simulation consisted of 5 separate simulations with different seeds and 100000 histories each. 5 seeds were used not only to be able to calculate a standard deviation for the range and full width at half maximum of each peak but also to protect against any error that could happen during said simulations, by doing several smaller simulations if any error occurs only the current simulation will be affected instead of rendering an entire simulation useless if a single large one was ran, (some of the simulations take a long time to be completed and the computer used at the time could crash). The TOPAS parameter files were setup in a way that the only necessary change to repeat the simulation was changing the energy of the beam.

Figure 5 shows that at the Bragg Peak zone both matRad and TOPAS beams are in close agreement which is excellent since this is the zone which will contribute the most to the total dose. The largest difference between the matRad beams and their equivalent TOPAS beams occurs at the entrance and plateau regions, especially for lower energies. This occurs since Monte Carlo simula-

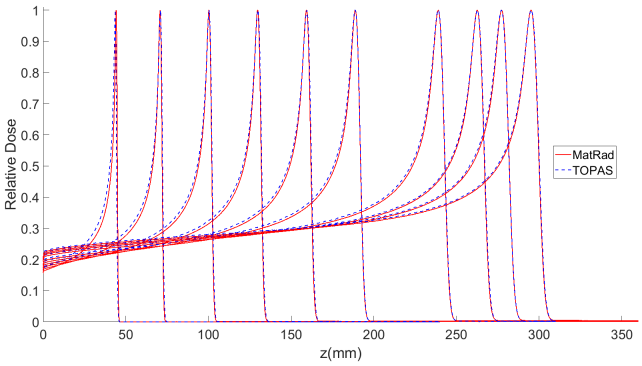

Figure 5: Comparison of depth dose distributions between MatRad beams of 73.41 MeV, 95.59 MeV, 116.36 MeV, 134.68 MeV, 151.44 MeV, 166.98 MeV, 191.38 MeV, 202.16 MeV, 208.72 MeV and 216.45 MeV and the corresponding beams simulated with TOPAS. Each beam is normalized to its maximum.

tions take into account scattering at the treatment head while analytical methods don't and this causes analytical methods to "lose" some particles leading to the lower dose at the entrance [14]. This is less of an issue than one would expect since this zone is less relevant to the overall plan. For lower energies it can, in a perfect scenario, influence a volume which is outside the patient and in the case that it influences the Planning Target Volume (PTV) there will be less particles and therefore a lower impact on the overall dose.

The average value of 0.4 mm for the difference in R80 and 1 mm for the difference in FWHM between the matRad beams and the simulated ones in TOPAS prove that in the zone close to the Bragg Peak the dose distribution of matRad and TOPAS beams are in close agreement. Therefore the parameters calculated through matRad can be used to simulate treatment plans with TOPAS, in principle, without significant differences between the two.

C. Box Phantom

After achieving a satisfying level of agreement between TOPAS and matRad for dose distributions for single beams, the following step was to move to a target volume. This section intends to verify if multiple beams can be combined to achieve a specific dose distribution in a target volume. The simplest option is a constant dose in a cubic water phantom. For these simulations an example included in matRad files, which can be seen in Figure 6 was used. It consists of box phantom CT including a defined region of interest (ROI) and isocenter. The phantom is a 160x160x160 voxel cube with a 3 mm resolution making it a 480x480x480 mm^3 cube. The ROI is a smaller 240x240x240 mm^3 cube made of water, which corresponds to the volume where dose was scored in the TOPAS simulation. The target region where the dose is

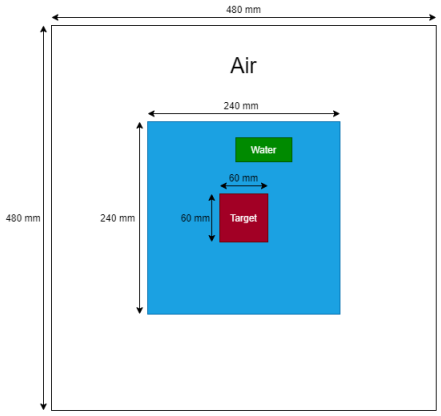

Figure 6: Geometry of the phantom for the box phantom simulations.

VOI	Priority	Optimization	Function	Penalty	Par 1	Par 2
Organ at Risk	2	O	So	100	Dose=$\frac{1}{12}$	
Target	1	O	Sd	800	Dose=1	
Target	1	C	Min DVH	800	Dose=1	Vol=0.95

Table I: Objectives (O) and constraints (C) for the optimization of dose to the box phantom simulation. So and Sd stand for squared overdosing and squared deviation, respectively, DVH stands for Dose Volume Histogram

supposed to be constant is a smaller 60x60x60 mm^3 cube placed in the middle of the 240mm side cube. Having imported the data, both the RTct and RTsegmentation variables are automatically defined, using the graphical user interface (GUI), the RTplan variable is easily created by choosing the radiation mode and corresponding machine, in this case the machine which was validated in section (II B), as well as the constraints and objectives, that can be seen in Table I, bixel width, gantry and couch angles, and finally scan spots locations which were 5 mm apart.

With the information from RTct, RTsegmentation and RTplan matRad can now generate the RTdij and RTarranjarnome variables and then taking into account all five variables matRad optimizes the weights for each beam and scan spot by minimizing the difference between objective and delivered dose to the ROI and generates the RTresult variable.

The next step is extracting the necessary information from matRad to be able to setup the required parameter files for the TOPAS simulations. The relevant parameters to be extracted are the energies of the used beams, the scan spots and weights for each beam and spot since others such as the size of the phantom or bin size are defined previously. These parameters are obtained and written into text files using a personalized script developed in MATLAB. Here is where TOPAS hierarchy control shows its advantages, knowing which beams are used, and having previously defined parameter files for each of the 86 beams in the matRad machine, the information of each beam is included in the simulation through one of TOPAS features. The ability to handle time varying

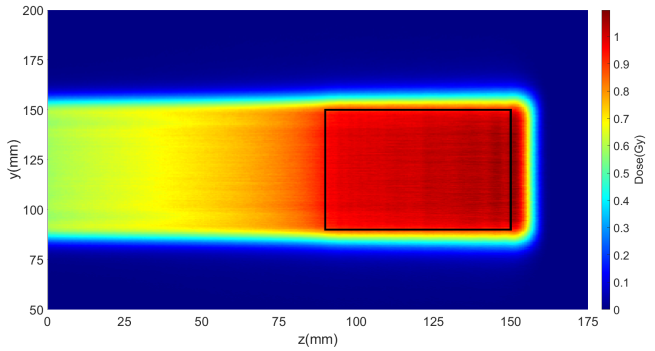

Figure 7: Dose delivered to the phantom in the box phantom plan. The black contour marks the target.

parameters is also very helpful in this situation, there are 169 scan spots, without time features 169 simulations would be needed, one for each scan spot and then the data would have to be combined, with time features the position of the source and weight of the beam can be changed to cover all 169 spots with each beam in a single simulation eliminating the need for further treatment of the data. The resulting dose for the simulation can be seen in Figure 7. The dose is normalized since there was no strict objective on how much dose should be delivered to the target, only dose to target in relation to dose to surrounding areas. This allowed simulations to be ran with only the number of histories necessary to achieve statistically relevant results and a smooth dose distribution instead of enough particles to achieve a certain dosage like it would have to be done for an actual plan with a specific Gy dose objective. Taking this into account, a satisfactory result was achieved, 93.4% of the target received at least 0.95 of the maximum dose and the dose had a range of 154.3 mm, 4.3 mm more than the target which ended at a depth of 150 mm, therefore tissues located downstream of the target would be spared.

D. Errors due to missassignments

The base phantom is the same as in section (II C), a cube entirely made of water. The two test phantoms are cubes of the same dimensions as the previous but with a material that has the same density and mean excitation energy as water but with the composition of muscle, in one case, and adipose on the other. The composition for both water-like muscle and water-like adipose tissue are taken from the Geant4 database.

The setup for the simulations is also the same as in section (II C) and can be seen in Figure 6, the simulations for the water-like muscle and water-like adipose tissue are ran with the weights for each beam and scan spot calculated in section (II C) as if the phantom was composed of water, this allows the assessment of the cumulative impact of material missassignment errors on the dose delivered to the phantom, if the cumulative error in this worst case scenario setup is not significant then it can be stated with confidence that sporadic errors will have a very small or negligible impact on the final dose.

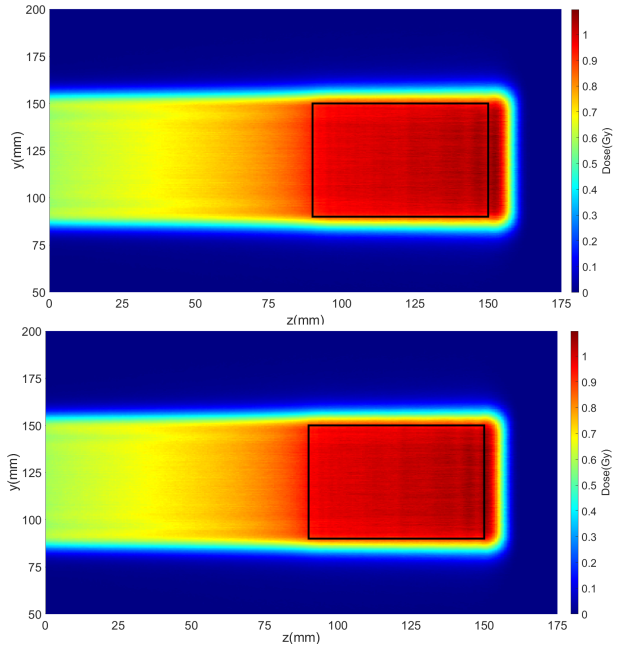

Figure 8: Dose delivered to the water-like muscle phantom on top and water-like adipose tissue phantom on the bottom. The black contour marks the target.

Material	R_{80}(mm)	Coverage(%)
Water	154.3	93.4
Water-like muscle	155.6	92.5
Water-like adipose tissue	153.8	94.3

Table II: Range and coverage for both the water and water-like materials phantoms plans

The dose distribution for the water-like muscle and water-like adipose tissue simulations are presented in Figure 8 and the ranges and coverage are in Table II, it can be observed that the differences in range are within the clinically accepted margins and the coverage is still above 92%. Based on this information it can be inferred that in this simple box phantom case errors in tissue assignment are not relevant to the final dose. It is important to mention that the coverage could be improved by continuing to tweak the constraints on the dose to achieve a more optimized dose delivery, of course this process would be extremely time consuming especially taking into account that the computer used at the time only had 4 threads, because of this the decision to accept this greater than 92% coverage was made due to time constraints and the need to move forward to the creation and evaluation of an actual treatment plan.

VOI	Priority	Optimization	Function	Penalty	Par 1
PTV	1	Objective	Squared deviation	800	Dose=1
GTV	1	Objective	Squared deviation	800	Dose=1
CTV	1	Objective	Squared deviation	800	Dose=1

Table III: Objectives and constraints for the optimization of the treatment plan

III. TREATMENT PLAN

A. Motivation

Following the successful validation of the MC beam model discussed in the previous chapter, a single beam proton treatment plan for a clinical case was created using matRad where the end goal is to once again assess the impact of composition missassignments in the patient CT on the delivered dose.

The treatment plan was developed for a brain tumour since head and neck cancers are the seventh most common type of cancer having 888 thousand estimated new cases in 2018 and causing 453 thousand deaths [15], also for the purpose of this work a smaller tumor was preferable instead of the even more common *medulloblastoma* due to computational time constraints.

B. Development

The CT of an oncologist patient with the structures already delineated by specialist was used. The first step to develop the treatment plan is analogous to section (II C), the CT data is imported to matRad which in turn generates the RTct and RTsegmentation variables. The proton treatment plan shared by the provider of the patient data alongside the CT used 3 different gantry and couch angles to achieve an uniform dose in the tumour while minimizing damage to adjacent healthy tissues, the most prominent (having more impact on total dose) being gantry and couch angles of 300^{o} and 90^{o}, respectively. In this work, the goal is not to necessarily simulate the most optimized treatment plan, but rather evaluating the effects of density missassignments in the CT. For this reason, a single beam configuration will be used in this chapter. This configuration still has to be able to deliver a conformal dose to the tumour while avoiding organs at risk since the results will be more relevant if acquired from a setup which could be used in a clinical setting.

A combination of a gantry angle of 270^{o} and a couch angle of 90^{o}, similarly to the 300^{o} and 90^{o} used in the provided plan, has the particle beams enter the body through the back of the head and avoids delivering dose to the eyes when optimized, which is shown in Figure 9. A set of constraints regarding the target were already provided alongside the CT and can be seen in Table III. Due to lack of data and clinical expertise, no constrains were set to the OARs, as it would be expected clinically.

As stated in section (II A) matRad is used as a stepping stone to then use Monte Carlo software TOPAS to simulate the plan using the parameters provided, naturally the next step is extracting these parameters to text files. This is done through a personalized MATLAB script similar to the one used in section (II C) (more complex as would be expected).

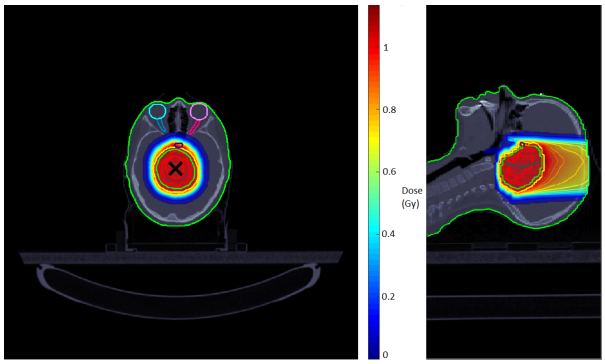

Figure 9: Axial (left) and sagital (right) views of the CT with the dose delivered through matRad optimization. No dose is delivered to either eye or optical nerve.

One file in particular is of extreme relevance to this work since it is what will allow the introduction and posterior assessment of errors in tissue assignment. In the Box Phantom case the phantom was created directly in TOPAS by defining its half lengths in the three dimensions and its material, in this section the Hounsfield Units in the CT must be converted into material densities and compositions for each voxel. The used method follows the work of [16] which details how HU units can be converted into mass density and composition.

TOPAS uses a slightly different formula for density as it needs to be applicable to the full range of HUs, equation 1.

$$\rho_{\mathrm{TOPAS}} = [\mathrm{Offset} + (\mathrm{Factor} \times (\mathrm{FactorOffset} + H)] \times \mathrm{DensityCorrection} \quad (1)$$

Where Offset, Factor and FactorOffset are calculated parameters and H is the Hounsfield Unit. While the densities are a continuous function, the compositions must be assigned beforehand and divided into bins, TOPAS once again closely follows of the work of Schneider et al [16]. The difference here is that the bin assigned to cortical bone is extended until 2995HU and there is an additional bin with the composition of titanium. With both a continuous function for densities and the division into bins for composition Hounsfield Units in the CT can now be converted into material properties for each voxel and the simulation can be ran.

C. Errors due to misassignments

In section (II D), the missassignments were introduced by changing the material of the phantoms, whereas that was not possible here since changing the entirety of the CT for these materials would not be realistic. Therefore the errors will be introduced by changing only the voxels in which either adipose tissue or muscle are located.

Changing the HU numbers directly on the CT would be hard since it would require previous knowledge of all the HUs in the CT, the more efficient solution is changing the way in which the HUs are transformed into densities and compositions, once again water-like muscle and water-like adipose tissue will be the introduced errors by in all voxels which would be composed of muscle or adipose tissue maintaining their respective compositions taken from the Geant4 database, but being assigned the density of water. Looking back at equation 1, which transforms HUs into densities, the final term (Density Correction) had not been discussed yet, this term is used to account for the differences between Geant4 and the used treatment planning system (TPS). This is the factor which allows the introduction of errors, in this work no specific TPS is used so the corrective term would be set to 1 for all HUs, to introduce the errors the corrective term is set in a way that forces the density of HUs corresponding to muscle or adipose to be that of water (1 g cm^{-3}). This is done through a personalized MATLAB scrpit which calculates the density assigned to each HU and then the necessary correction, which is afterwards converted into a parameter in the correct form needed to be introduced into TOPAS. The correction is applied from -98 HU (adipose 3) and 77 HU (Skin 3) which set the boundaries for adipose on the low end and muscle on the top end (Table IV).

			Elemental weights (%)						
Tissue	**HU**	**ρ(g cm^{-3})**	**H**	**C**	**N**	**O**	**P**	**Ca**	**Others**
adipose 3	-98	0.93	11.6	68.1	0.2	19.8	0	0	0.3
Skin 3	77	1.09	10.1	15.8	3.7	69.5	0.1	0	0.8

Table IV: HU, densities and compositions of the relevant materials. Adapted from [16].

D. Results

The dose delivered to both the unaltered HU conversion and corrected HU conversion to introduce errors can be seen in 2 different views, an axial view and a sagital view seen in Figure 10. The differences in range are very subtle and nigh impossible to see in these different views. In order to calculate the differences in range due to missassignments in the CT, the sagital plane was chosen as it provides the better of the dose. The calculations are made in the Beam Eye View (BEV) and calculate for all relevant X and Y around the isocenter the range of dose for that specific straight line of voxels, this is where the decision to have the beams placed at 270º instead of 300º comes into fruition as if the beam was oblique it would greatly complicate the calculations.

In these calculations, the differences in range in the boundaries were neglected. The boundaries are associated with a high degree of uncertainty and the values there are may not be representative of the errors induced by missassignments in the CT. The ranges for each XY pair around the isocenter are depicted in Figure 11 and the difference between ranges for the simulations without and with introduction of the missassignment errors can be seen in Figure 12. The average difference for the ranges defined as $R80_{corrected}$-R80 was 3.5 mm with a standard deviation of 0.4 mm, 96.8% of the voxels had a difference greater than 0, the fact that the differences in range have, in large majority, the same sign is a good sign that the changes in the HU conversion method were correctly introduced since the differences are consistent.

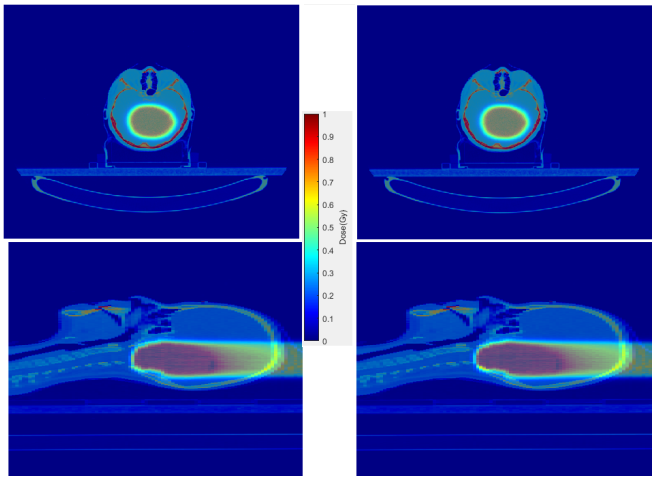

Figure 10: Comparison of the dose delivered to the patient, seen from the axial plane on top and sagital plane on the bottom. Simulations without correction on the left and simulations with the correction on density to introduce missassignments on the right.

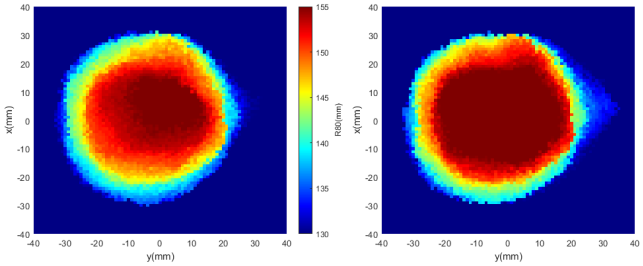

Figure 11: R_{80} for each X and Y, in the Beam Eye View, pair voxels for the simulation without introduction of errors on the left and the simulation with introduction of errors on the right. Distances are relative to the isocenter.

IV. CARBON IONS

A. Motivation

Particle beam radiotherapy can also be delivered using carbon ions. Interactions of ^{12}C ion beams with matter are similar to those of proton beams, the differences lie in the heavier mass of carbon ions and its higher charge as well. There are 2 main advantages ^{12}C ion beams have that make its study interesting. Firstly, their penum-

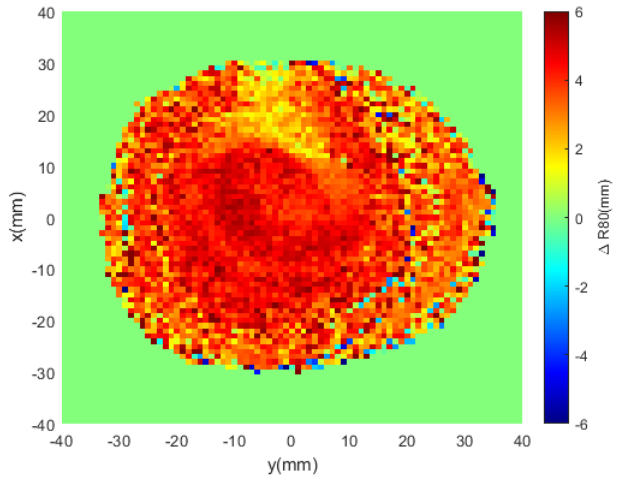

Figure 12: Differences in $_{80}$ for each X and Y, in the Beam Eye View, pair voxels between the simulation without introduction of errors and the simulation with introduction of errors. Distances are relative to the isocenter.

bra is sharper than in proton therapy, in proton beams the penumbra increases as the range increases while for carbon ions it remains almost constant [17].

The other advantage involves the Relative Biological Effectiveness (RBE), for protons RBE can be approximated to 1.1 without significant errors [18], while for carbon ions it varies, RBE for ^{12}C ions increases until the Bragg Peak where it reaches its maximum and then decreases. This advantage comes from the fact than since RBE is at its highest at the Bragg Peak less physical dose will need to be delivered which eases the load on the patient while retaining the same biological damage to tumour cells. But this also brings a downside, since RBE varies the planning of the treatment can be significantly more complex, as this variation in RBE must be taken into account and the physical dose has to be adjusted to ensure an homogeneous dose covers the tumour.

Another characteristic that must be taken into account is the fragmentation tail that appears in carbon ion beams, this happens because secondary particles are created during nuclear interactions with nucleus in the traversed medium, some of these secondary particles travel non negligible distances beyond the range of the primary beam.

The main goal for this chapter was to once again study the impact of missassignment errors of the CT on the dose delivered to the patient.

B. Validation

As in section (II B), the first step to be able to develop the treatment plan is to validate the beams in the chosen matRad machine, the setup is also the same as in that section.

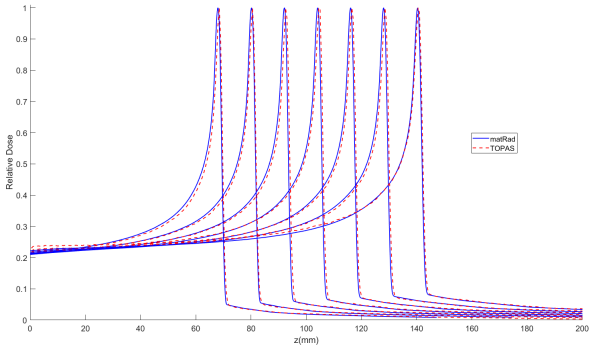

Figure 13: Comparison of depth dose distributions between matRad beams of 178.28 MeV/u, 195.18 MeV/u, 211.19 MeV/u, 226.46 MeV/u, 241.03 MeV/u, 255.17 MeV/u and 268.86 MeV/u, from left to right, and the corresponding beams simulated in TOPAS. Each beam is normalized to its maximum.

Carbon ions having higher mass and higher atomic numbers interacts more strongly with the traversed medium, this, alongside with the formation of the fragmentation tail which forces particles to be tracked for greater depths, causes the MC simulations for ^{12}C ion beams to be much more time consuming (about 50 times more time consuming for the same setup and number of histories), the process of validation for the proton beams was already the most time consuming section of the work so doing the same here would be impossible due to time constraints, even with the upgraded computer. To work around this issue, the box phantom chapter was skipped and the validation was performed only for the beams which would be used in the simulation of the treatment plan, which reduced the amount of validated beams from the 121 included in the machine to 21 used for the plan ranging from 178.28 MeV/u to 277.77 MeV/u and covering ranges from 68.9 mm to 149.8 mm.

Figure 13 shows that the TOPAS beams are in close agreement with the matRad beams, the figure also shows the very noticeable fragmentation tails in contrast to Figure 5 in which proton beams did not have dose after the Bragg Peak, it is also very noticeable that the FWHM of the carbon ion beams stays almost constant, varying from 6.0 mm to 7.5 mm while for protons of comparable range it varied from 6.2 mm to 13 mm.

Having an average Δ R80 of 0.2 mm and all values below 0.5 mm, which is the size of one voxel, corroborates the visual evidence seen in Figure 13 that the TOPAS beams have a identical behaviour to their corresponding beams in the matRad machine therefore the parameters calculated through matRad can be used to simulate treatment plans with TOPAS, in principle, without significant differences between the two.

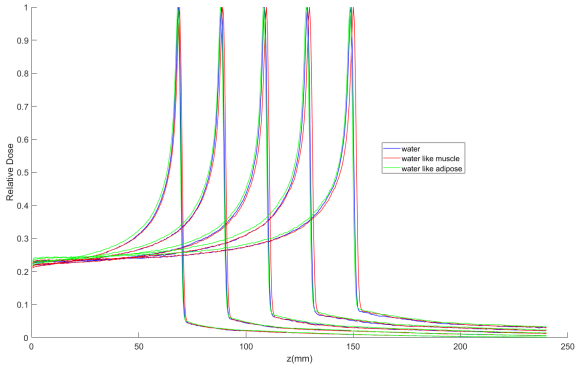

Figure 14: Comparison Comparison of depth dose distributions between beams of 178.28 MeV/u, 205.95 MeV/u, 231.34 MeV/u, 255.17 MeV/u and 277.77 MeV/u, from left to right, travelling through water, water-like muscle and water-like adipose tissue phantoms. Water like muscle and water like adipose tissue are, respectively, materials with the composition of muscle or adipose tissue but with the density and mean excitation energy of water. Each beam is normalized to its maximum.

C. Errors due to missassignments

The initial goal was to develop a treatment plan for carbon ions, hence the validation on the previous chapter, but due to time constraints (simulations with the same level of statistical relevance as the ones performed for the proton treatment plan would take upwards of 800 days) that was not possible. Because of this the analysis for carbon ion beams was reduced to comparing the ranges and FWHMs of the validated beams which would be used on the treatment plan trough phantoms of water, water-like muscle and water-like adipose tissue.

In Figure 14, the behaviour of 5 beams of different energies can be seen, the dose profile near the entrance and at the fragmentation tails is somewhat rocky, once again this is due to time constraints, the number of histories for each simulation had to be reduced so that the data could be acquired in a reasonable amount of time, despite this in the more relevant area around the Bragg Peak the dose is still smooth.

The differences in range are very similar to the ones obtained for proton beams of comparable ranges, for a range close to 105 mm the differences for protons were 0.8 mm and 0.4 mm for water-like muscle and water-like adipose tissue, respectively, and for ^{12}C ions these differences were 0.7 mm and 0.4 mm.

V. COMPARISON OF EACH THERAPY

Having simulated the behaviours of beams of both proton and ^{12}C ions and a treatment plan for protons all while analyzing and quantifying the errors due to tissue missassignments in the CT a comparison between each therapy can be made, also including photon therapy, looking at different parameters. A summary of this comparison can be seen in Table V.

Particle	Photons	Protons	Carbon Ions
Planning (difficulty)	Easiest	Medium	Hardest
Penumbra(<15 cm depth)	Worst	Medium	Best
Penumbra (>15 cm depth)	Medium	Worst	Best
Distal Falloff	——	Sharp	Sharpest
Relative biological effectiveness	1	0.7-1.6	1-3.5
Time consumed	Lower	Medium	Highest
Potential ceiling	Lower	High	Highest
Price	Cheapest	Medium	Most expensive

Table V: Comparison between characteristics for each particle therapy.

Photons are the easier particle to plan as they interact less with the body while carbon ions are the most complex as it is needed to take into account both the fragmentation tail and the varying values of RBE. ^{12}C ion beams have the smallest penumbra, ^{12}C ions are heavier than protons so the effects of MCS have less effect on the sharpness of the beam, while photon beams have the highest (until about 15 cm where proton beams, due to MCS interaction deteriorating the sharpness of the beam, see their penumbra raise above the one of photons). Carbon ions distal falloff is also sharper than the one of protons and the FWHM of carbon stays almost constant as the range increases while for protons it increases much more prominently. The differences due to missassignments in the CT for generic beams of comparable ranges were nearly similar for proton and carbon ions. Photons have lower RBE while carbon ions have the highest, meaning carbon ion beams will do more damage to both tumour and healthy cells. Despite making it more effective, it also becomes more complex to plan as a mistake in planning will lead to higher damage to healthy tissues.

It is important to consider is the potential for improvement in each therapy. It has been argued that proton therapy has a higher ceiling than conventional radiotherapy[19]. For the reasons previously listed it can be conclude that carbon ion therapy has an even higher potential.

In terms of cost, heavier particles are harder to accelerate therefore ^{12}C ion therapy will be the most expensive. Carbon ion therapy is also the most time consuming in terms of planning a treatment, not only from the fact that the planning itself is more complex but also if MC simulations are to be used said simulations take much longer than a similar situation for protons.

VI. CONCLUSIONS AND FUTURE WORK

Uncertainties in proton therapy are much more severe than in photon radiotherapy due to the finite range of the particles. Missassignment errors in the CT of a patient are a cause for these uncertainties in range.

Under this thesis, the impact of these errors on the range of the dose was calculated for a variety of configu-

rations using Monte Carlo simulations.

The first setup were generic proton beams with energies from 80 MeV to 240 MeV travelling through a homogeneous cubic phantom. The errors were introduced by changing the composition of the phantom from water to water-like muscle and water-like adipose tissue, these virtual tissues have the the composition of muscle or adipose tissue, respectively, but are assigned the density of water. The differences in range were all below 1% and grow as the energy rises, as expected since the beam travels through a greater depth and the differences in material have a larger impact on the loss of energy.

The process of creating a treatment plan with particle therapy requires defining several parameters that follow detailed clinical protocols which depend on the type of particle, beam, machine and even center. The treatment plan is calculated by complex algorithms that manipulate parameters such as spot position and size as well as beam energy and weight to achieve the best possible dose to the target while minimizing dose delivered to the surrounding volumes. To calculate these parameters matRad, an open source code based on MATLAB, was used. The beams to be used in TOPAS were validated with an average range difference of (0.4±0.3) mm.

A treatment for a brain tumour of a pediatric patient was developed. In this chapter segmentation errors were introduced by modifying the method of conversion from Hounsfield Units (HU), in the CT to densities and compositions so that voxels of the CT with either muscle or adipose kept their composition but were assigned the density of water. This was done by introducing a correction factor to the density formula.

The average difference in range due to these errors was 3.5 mm (2.6% of the range) with a standard deviation of 0.4 mm. This value of 2.6% is higher than the estimation made in [13] of 1.7% but it must be kept in mind that the value obtained here was the worst case scenario where the errors were introduced into all voxels. If the margins for a treatment plan are to be defined in the most conservative way possible the contribution due to missassignments in the CT numbers should be 3.9 mm (the upper value of the average plus the standard deviation).

The same treatment plan was to be developed for carbon ions so the necessary beams were validated and had an average range difference of (0.2±0.1)mm.

Due to time constraints caused by the long computational time of carbon ion beams the treatment plan was not able to be developed, despite this taking into account both the validation and the physics of these beams it is expected that the difference in range would be similar or inferior to the one calculated for protons.

A comparison was made between each therapy where it was concluded that while carbon ion therapy has the highest potential to deliver a uniform dose alongside being easier on the patient, this therapy is also the most expensive as well as most complex and time consuming to plan.

Because of time limitations the simulation for the treatment plan using carbon ions was not possible therefore future work could include this simulation as well similar simulations for different sized tumours located in different areas since the differences in range will be affected both by the size and location of the tumour and the traversed tissues. If someone else was to further develop this research, it should be noted that a barrier would be the development of the scripts that both create the parameter files and analyze the data. This work took place "behind the scenes" but was very complex and integral to the thesis.

[1] "Cancer management," https://www.iarc.fr/wp-content/uploads/2018/07/wcr-6.pdf (2020).

[2] "Cancer fact sheets," https://gco.iarc.fr/today/data/factsheets/cancers/39-All-cancers-fact-sheet.pdf (2020).

[3] "Terapies," https://www.iarc.fr/wp-content/uploads/2018/07/wcr-6.pdf (2020).

[4] S. Tyldesley, G. Delaney, F. Foroudi, L. Barbera, M. Kerba, and W. Mackillop, International Journal of Radiation Oncology*Biology*Physics **79**, 1507 (2011).

[5] "Portugal cancer fact sheets," https://gco.iarc.fr/today/data/factsheets/populations/620-portugal-fact-sheets.pdf (2020).

[6] "Facilities in operation," https://www.ptcog.ch/index.php/facilities-in-operation (2020).

[7] Saaidi and C. E. Moursly, "Monte carlo study of photon dose distributions produced by 12 mv linear accelerator," (2018).

[8] A. Lomax, "Charged particle therapy: The physics of interaction," (2009).

[9] S. A. et al, Nuclear Instruments and Methods in Physics Research Section A: Accelerators, Spectrometers, Detectors and Associated Equipment **506**, 250 (2003).

[10] "Topas mc," http://www.topasmc.org/ (2012).

[11] J. Perl, J. Shin, J. Schümann, B. Faddegon, and H. Paganetti, Medical Physics **39**, 6818 (2012).

[12] T. Bortfeld, Medical Physics **24**, 2024 (1997).

[13] H. Paganetti, Physics in Medicine and Biology **57**, R99 (2012).

[14] B. Bednarz, J. Daartz, and H. Paganetti, Physics in Medicine and Biology **55**, 7425 (2010).

[15] "World cancer report," https://publications.iarc.fr/586 (2020).

[16] W. Schneider, T. Bortfeld, and W. Schlegel, Physics in medicine and biology **45**, 459 (2000).

[17] S. et al, "Proton vs carbon ion beams in the definitive radiation treatment of cancer patients," (2010).

[18] H. Paganetti and P. van Luijk, Seminars in Radiation Oncology **23**, 77 (2013).

[19] H. Paganetti, C. X. Yu, and C. G. Orton, Medical Physics **43**, 4470 (2016).